Biosynthesis of Antinutritional Alkaloids in Solanaceous Crops Is Mediated by Clustered Genes

M. Itkin *et al.*

Science **341**, 175 (2013);
DOI: 10.1126/science.1240230

fig. S13A and fig. S14). Consistent with its partially constitutive activity, the mutant was still responsive to flagellin (Fig. 3D).

HD2 exists in all NLRs (*8*), but whether and how it contributes to NLR autoinhibition remain unknown. The HD2 of mNLRC4ΔCARD is positioned differently from that of the inactive Apaf-1 (fig. S9) but similarly to the WHD of CED-4 that is involved in the formation of the CED-4 apoptosome (*24*) (fig. S11A). These structural observations suggest that HD2 may have a role in mNLRC4 autoinhibition. Consistent with this, the mNLRC4 mutant lacking HD2 and LRR domains was more efficient at activating IL-1β than the mutant lacking the LRR domain only (Fig. 3B). HD2 contacts α8 from NBD (Fig. 4, A and B), a conserved structural component involved in oligomerization of STAND family members (*8*, *21*, *24*). Mutation of Arg^{288} but not Arg^{285} of α8 to alanine abrogated flagellin-induced IL-1β activation (Fig. 4C and fig. S13C), supporting a critical role for α8 in mNLRC4 activation. Failure of the R288A (R, Arg) protein to activate IL-1β was not caused by its defect in folding or in interaction with mNAIP5 (fig. S15).

The NBD-HD2 interaction is mainly mediated by packing of α8 against α20 and the loop C-terminal to α21 (Fig. 4B). Ser^{485} from α20 and Gly^{520} from the loop act as supporting points for the packing, which is further strengthened by Arg^{285} wedged between the loop and α20. The interactions with the HD2 domain result in steric masking of α8. As anticipated, the mutants S485R and G520Y (S, Ser; G, Gly) constitutively activated IL-1β (Fig. 4C, and figs. S13B and S14) but were still responsive to flagellin (Fig. 4C). The variant carrying the mutations of Y617A and G520Y became more efficient for ligand-independent IL-1β activation than either of the single mutants (Fig. 4D), suggesting a cooperative inhibition of mNLRC4 by the LRR and HD2 domains. Together, our data show that HD2 acts as an autoinhibitory domain by negatively regulating the function of the conserved α8 in mNLRC4 activation.

The effects generated by the mutation H443L (Fig. 2, C and D) demonstrate the important role of the His^{443}-ADP interaction in NLRC4 autoinhibition. Given the conserved histidine (*28*) from other NLR proteins, some of the disease-related mutations (*2*–*4*) in the NLR proteins are expected to perturb a similar interaction and result in their constitutive activation. The LRR-mediated NLRC4 inhibition is reminiscent of CED-4 inhibition by CED-9 in which CED-9 blocks CED-4 oligomerization (*25*). In addition, the first WD40 domain in the inactive Apaf-1 overlaps with the LRR domain of mNLRC4 and an adjacent protomer of a lateral dimer from the Apaf-1 apoptosome (*26*) (fig. S16).

The close locations to a potential ligand-binding site (fig. S17A) make it possible for the HD2-NBD and the LRR-NBD interfaces to be perturbed upon ligand binding. The extensive WHD-HD2 (Fig. 1B) and HD2-LRR interactions (fig. S8) appear not sufficiently labile to be disrupted to allow substantial conformational changes in one domain with respect to the other two. Additionally, phosphorylation of Ser^{533} (pS533) (fig. S18), which is critical for assembly of the mNLRC4 inflammasome (*15*), acts to stabilize the HD2-LRR interaction. Thus, ligand binding may disengage the three domains as a whole from the NBD, rendering it accessible to a second NLRC4 molecule for oligomerization (fig. S17B). pS533 can have a role in this process through unknown mechanisms. Regardless of the mechanism of intermediates, it seems that ligand binding allosterically activates the assembly of the NLRC4 inflammasome.

References and Notes

1. J. von Moltke, J. S. Ayres, E. M. Kofoed, J. Chavarría-Smith, R. E. Vance, *Annu. Rev. Immunol.* **31**, 73 (2013).
2. L. Franchi, R. Muñoz-Planillo, G. Núñez, *Nat. Immunol.* **13**, 325 (2012).
3. V. A. Rathinam, S. K. Vanaja, K. A. Fitzgerald, *Nat. Immunol.* **13**, 333 (2012).
4. T. M. Ng, J. Kortmann, M. D. Monack, *Curr. Opin. Immunol.* **25**, 34 (2013).
5. T. Strowig, J. Henao-Mejia, E. Elinav, R. Flavell, *Nature* **481**, 278 (2012).
6. H. Wen, J. P. Ting, L. A. O'Neill, *Nat. Immunol.* **13**, 352 (2012).
7. L. Zitvogel, O. Kepp, L. Galluzzi, G. Kroemer, *Nat. Immunol.* **13**, 343 (2012).
8. O. Danot, E. Marquenet, D. Vidal-Ingigliardi, E. Richet, *Structure* **17**, 172 (2009).
9. F. Martinon, K. Burns, J. Tschopp, *Mol. Cell* **10**, 417 (2002).
10. B. Faustin *et al.*, *Mol. Cell* **25**, 713 (2007).
11. J. A. Duncan *et al.*, *Proc. Natl. Acad. Sci. U.S.A.* **104**, 8041 (2007).
12. J. L. Poyet *et al.*, *J. Biol. Chem.* **276**, 28309 (2001).
13. E. F. Halff *et al.*, *J. Biol. Chem.* **287**, 38460 (2012).
14. E. M. Kofoed, R. E. Vance, *Nature* **477**, 592 (2011).
15. Y. Qu *et al.*, *Nature* **490**, 539 (2012).
16. L. Franchi *et al.*, *Nat. Immunol.* **7**, 576 (2006).
17. E. A. Miao *et al.*, *Nat. Immunol.* **7**, 569 (2006).
18. A. B. Molofsky *et al.*, *J. Exp. Med.* **203**, 1093 (2006).
19. Y. Zhao *et al.*, *Nature* **477**, 596 (2011).
20. E. A. Miao *et al.*, *Proc. Natl. Acad. Sci. U.S.A.* **107**, 3076 (2010).
21. J. P. Erzberger, J. M. Berger, *Annu. Rev. Biophys. Biomol. Struct.* **35**, 93 (2006).
22. S. J. Riedl, W. Li, Y. Chao, R. Schwarzenbacher, Y. Shi, *Nature* **434**, 926 (2005).
23. T. F. Reubold, S. Wohlgemuth, S. Eschenburg, *Structure* **19**, 1074 (2011).
24. S. Qi *et al.*, *Cell* **141**, 446 (2010).
25. N. Yan *et al.*, *Nature* **437**, 831 (2005).
26. S. Yuan, M. Topf, T. F. Reubold, S. Eschenburg, C. W. Akey, *Biochemistry* **52**, 2319 (2013).
27. S. Yuan *et al.*, *Structure* **19**, 128 (2011).
28. M. Proell, S. J. Riedl, J. H. Fritz, A. M. Rojas, R. Schwarzenbacher, *PLoS ONE* **3**, e2119 (2008).

Acknowledgments: We thank P. Schulze-Lefert for critically reading the manuscript, F. Yu and J. He at Shanghai Synchrotron Radiation Facility BL17U1 for data collection, L. Yu for helpful suggestions on culturing 293T cells, G. He from Y. Yan's laboratory assistance with CD, and J. Yang from F. Shao's laboratory for suggestions on cell-based assays. The coordinates and structural factors for mNLRC4ΔCARD have been deposited in the Protein Data Bank (PDB) with the accession code 4KXF. This research was funded by the National Outstanding Young Scholar Science Foundation of China (20101331722) and State Key Program of National Natural Science of China (31130063) to J. Chai.

Supplementary Materials

www.sciencemag.org/cgi/content/full/science.1236381/DC1
Materials and Methods
Figs. S1 to S18
Table S1
References (*29*–*39*)

11 February 2013; accepted 30 May 2013
Published online 13 June 2013;
10.1126/science.1236381

Biosynthesis of Antinutritional Alkaloids in Solanaceous Crops Is Mediated by Clustered Genes

M. Itkin,[1]* U. Heinig,[1] O. Tzfadia,[1] A. J. Bhide,[1,2] B. Shinde,[1,2] P. D. Cardenas,[1] S. E. Bocobza,[1] T. Unger,[4] S. Malitsky,[1] R. Finkers,[5] Y. Tikunov,[5] A. Bovy,[5] Y. Chikate,[1,2] P. Singh,[1,2] I. Rogachev,[1] J. Beekwilder,[5] A. P. Giri,[1,2] A. Aharoni[1]†

Steroidal glycoalkaloids (SGAs) such as α-solanine found in solanaceous food plants—as, for example, potato—are antinutritional factors for humans. Comparative coexpression analysis between tomato and potato coupled with chemical profiling revealed an array of 10 genes that partake in SGA biosynthesis. We discovered that six of them exist as a cluster on chromosome 7, whereas an additional two are adjacent in a duplicated genomic region on chromosome 12. Following systematic functional analysis, we suggest a revised SGA biosynthetic pathway starting from cholesterol up to the tetrasaccharide moiety linked to the tomato SGA aglycone. Silencing *GLYCOALKALOID METABOLISM 4* prevented accumulation of SGAs in potato tubers and tomato fruit. This may provide a means for removal of unsafe, antinutritional substances present in these widely used food crops.

Our demand for more and better food continues to increase. Improved nutritional qualities, as well as removal of antinutritional traits, are needed. Various approaches have been used to add nutritional qualities to food crops. We focus here on reducing the level of endogenous, antinutritional factors in existing crops (*1*). Antinutritional substances range from lethal toxins to compounds that disrupt digestion and nutrient absorption (*2*). In the course of crop domestication, levels of antinutrients were reduced by selection and/or breeding, although some of such substances remain in the general food source. In addition, wild germplasm, which can be useful as a source of

novel traits such as pathogen resistance, may also be complicated by co-occurrence of antinutritional compounds that need to be removed. Current technologies include extensive backcrossing, which can be a slow and imperfect process (*3*).

Steroidal glycoalkaloids (SGAs), found in staple vegetable crops such as potato (*Solanum tuberosum*) and tomato (*S. lycopersicum*), are a class of antinutritional substances that remain in our food chain and daily diet (*4*). The glycoalkaloids α-solanine (*5*) and α-chaconine are the principal toxic substances in potato. These SGAs cause gastrointestinal and neurological disorders and, at high concentrations, may be lethal to humans. Mechanisms of toxicity include disruption of membranes and inhibition of acetylcholine esterase activity (*6*). For this reason, total SGA levels exceeding 200 mg per kg fresh weight of edible tuber are deemed unsafe for human consumption (*7*). SGA biosynthesis requires genes encoding uridine 5′-diphosphate (UDP)–glycosyltransferases (UGTs) that decorate the steroidal alkaloid (SA) skeleton with various sugar moieties (*8*, *9*). The tomato GLYCOALKALOID METABOLISM 1 (GAME1) glycosyltransferase, a homolog of the potato SGT1 (*8*), catalyzes galactosylation of the alkamine tomatidine (*9*). Cholesterol is the proposed common precursor for biosynthesis of both steroidal alkaloids (SAs) and non-nitrogenous steroidal saponins (STSs) (Fig. 1 and fig. S1) (*10*). Conversion of cholesterol to the alkamine SA should require several hydroxylation, oxidation, and transamination reactions (*10*). Here, we identify genes encoding enzymes performing the conversion of cholesterol to SGAs and use them to engineer *Solanaceae* plants with reduced SGA content.

To discover genes associated with SGA biosynthesis, we carried out coexpression analysis using transcriptome data from tomato and potato plants (*11*). Sixteen genes from each species were coexpressed with *GAME1*/*SGT1* (Fig. 2). One of these genes, which we named *GLYCOALKALOID METABOLISM 4* (*GAME4*), encodes a member of the 88D subfamily of cytochrome P450 proteins (fig. S2). *GAME4* and *GAME1*/*SGT1* display a very similar expression profile in tomato and potato (fig. S3, B and C, and fig. S4). We then discovered that the *GAME1*/*SGT1* and *GAME4* genes in tomato and potato are positioned in chromosomes 7 and 12, respectively, such that they are physically next to several of their coexpressed genes (Fig. 3).

A cluster of *GAME1*/*SGT1* coexpressed genes spans a ~200 kilo–base pair genomic region on chromosome 7. Together with *GAME1*, the tomato cluster is composed of seven coexpressed genes. These include three UDP-glycosyltransferases [*GAME2* (termed *SGT3 in potato*), *GAME17*, and *GAME18*], a cytochrome P450 of the 72A subfamily (*GAME6*), a 2-oxoglutarate–dependent dioxygenase (*GAME11*), and a cellulose synthase-like protein. It appears that in potato this cluster contains five coexpressed genes as it lacks homologs of the tomato GAME17 and GAME18 UDP-glycosyltransferases. We performed enzyme activity assays with the four recombinant clustered tomato UDP-glycosyltransferases. GAME17 and GAME18 exhibited UDP-glucosyltransferase activity when incubated with tomatidine galactoside (T-Gal) and γ-tomatine (T-Gal-Glu) as a substrate, respectively, whereas GAME2 was shown to have a UDP-xylosyltransferase activity when incubated with β1-tomatine (T-Gal-Glu-Glu) as a

[1]Department of Plant Sciences, Weizmann Institute of Science, Rehovot 76100, Israel. [2]Plant Molecular Biology Unit, Division of Biochemical Sciences, Council of Scientific and Industrial Research–National Chemical Laboratory, Pune 411008, MS, India. [3]Department of Plant Pathology and Microbiology, The Robert H. Smith Faculty of Agriculture, Food and Environment, The Hebrew University of Jerusalem, Rehovot 76100, Israel. [4]Israel Structural Proteomics Center, Weizmann Institute of Science, Rehovot 76100, Israel. [5]Plant Research International, Wageningen University and Research Centre, POB 16, 6700 AA, Wageningen, Netherlands.

*Present address: Agricultural Research Organization, The Volcani Center, Bet Dagan 50250, Israel.
†Corresponding author. E-mail: asaph.aharoni@weizmann.ac.il

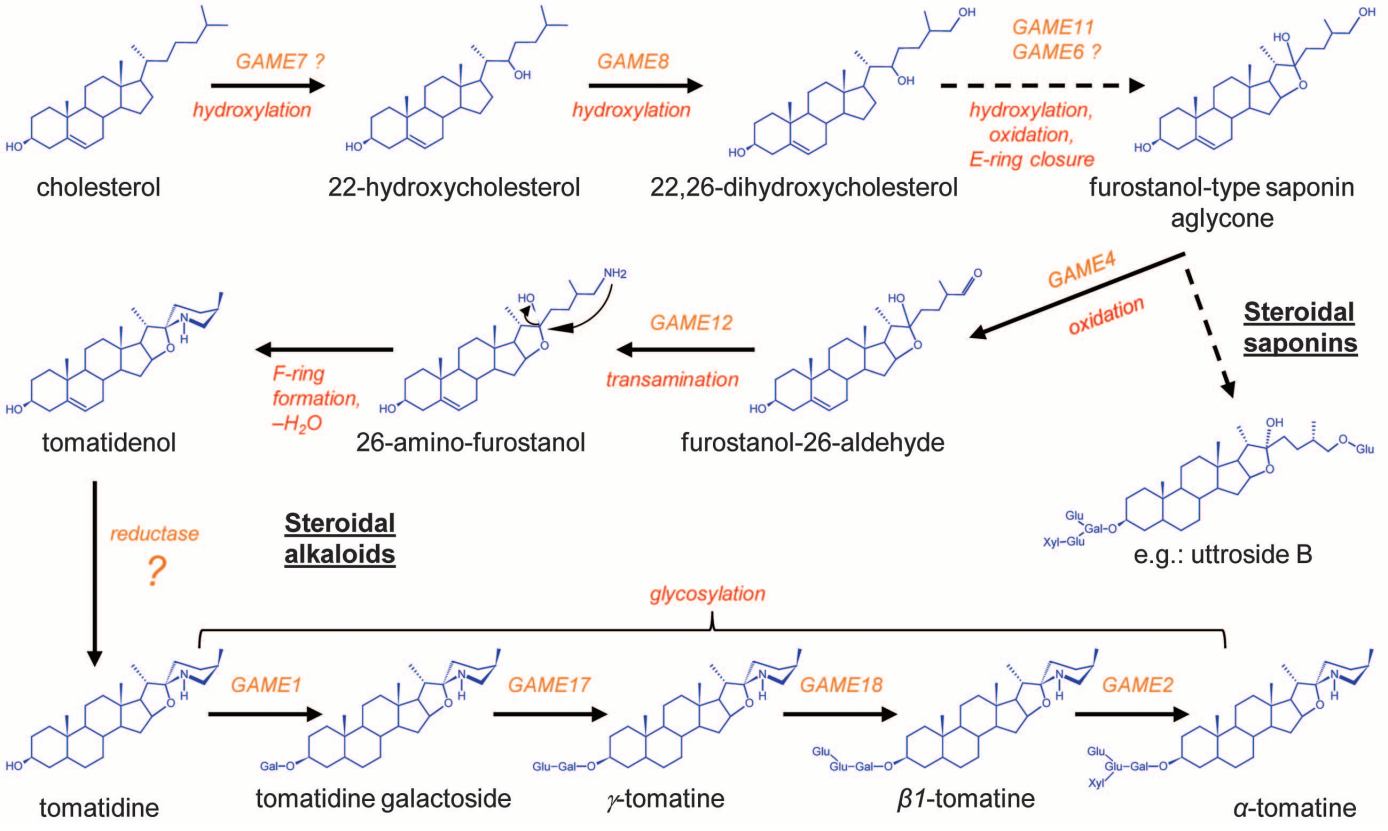

Fig. 1. Biosynthesis of steroidal alkaloids and saponins in the triterpenoid biosynthetic pathway in *Solanaceae* plants. Suggested biosynthetic pathway from cholesterol toward α-tomatine. Dashed and solid arrows represent multiple or single enzymatic reactions in the pathway, respectively. The proposed activity of *GAME1*, *GAME4*, and *GAME8* was supported by investigating transgenic plants; of *GAME11*, *GAME12*, and *GAME18* by VIGS assays; and of *GAME1*, *GAME17*, *GAME18*, and *GAME2* by activity assays of the recombinant enzymes.

substrate (Fig. 4, F to H, and fig. S5). GAME1 was previously shown to act as a tomatidine UDP-galactosyltransferase in tomato (*9*). When incubating the four recombinant UGT enzymes in a single test tube, with tomatidine, and all glycoside donors (UDP-galactose, -glucose and -xylose), we observed the accumulation of the final SGA product, α-tomatine (Fig. 4I and fig. S5). The role of *GAME18* in creating the tetrasaccharide moiety

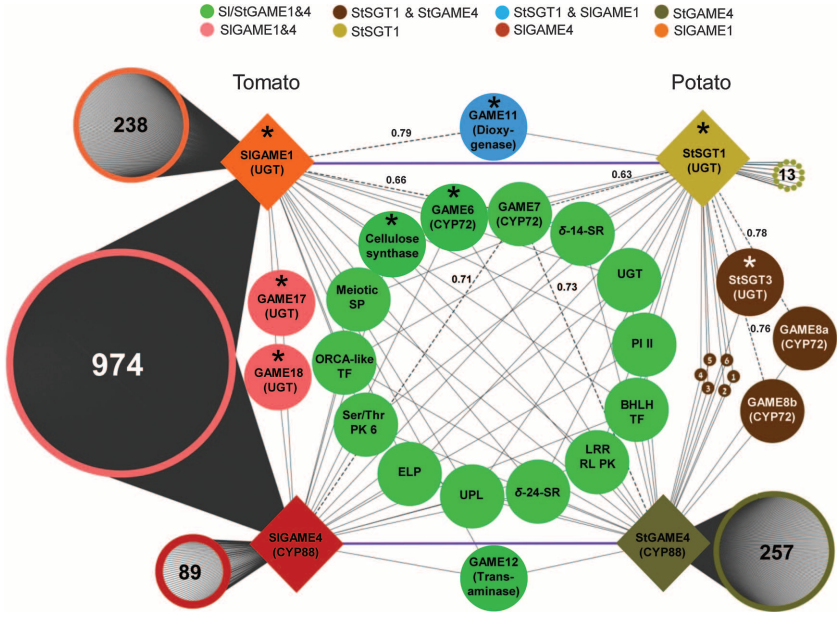

Fig. 2. Steroidal alkaloids gene discovery through coexpression network analysis in *Solanaceae* plants. Shared homologs of coexpressed genes for "bait-genes" from tomato (*SlGAME1 and SlGAME4*) and potato (*StSGT1 and StGAME4*). Continuous [correlation coefficient (r) > 0.8] and dashed (r > 0.63) lines connect coexpressed genes. *, located in the tomato or potato chromosome 7 cluster. St, *Solanum tuberosum*; Sl, *S. lycopersicum*. Color background of gene names corresponds to the bait with which they were found to be coexpressed (as above). (For more details, see tables S1 to S10.) SP, serine proteinase; PI, proteinase inhibitor; UPL, ubiquitin protein ligase; ELP, extensin-like protein; PK, protein kinase; SR, sterol reductase; RL, receptor-like.

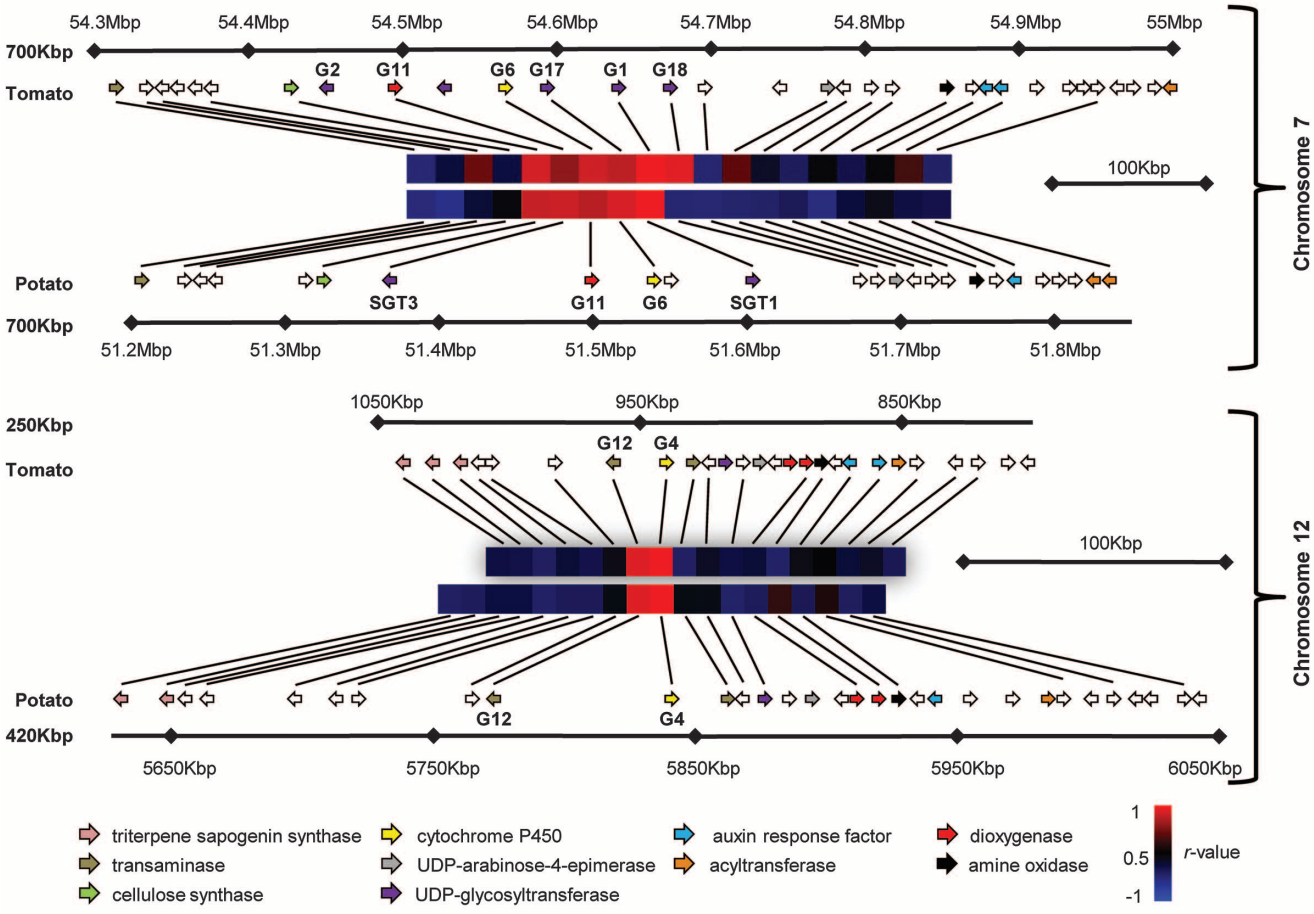

Fig. 3. Schematic map of genes identified in the duplicated genomic regions in tomato and potato and their coexpression. Coexpression with *GAME1/SGT1* (chromosome 7) and *GAME4* (chromosome 12) as baits in either potato or tomato are presented in the form of a heat map (table S12). Specific gene families are indicated by colored arrows, whereas members of other gene families are shown by white arrows. Note the homology in genes flanking the high-coexpression regions and positioned in a matching sequence along the genome, suggesting a common origin of the regions on both chromosomes (see fig. S11).

of α-tomatine was supported by virus-induced gene silencing (VIGS) assays as *GAME18*-silenced fruit accumulated γ-tomatine that was not present in the control sample (fig. S6, A to E). Analysis of the tomato leaves, silenced (VIGS) in GAME11, a putative dioxygenase in the cluster, revealed a significant reduction in α-tomatine levels and accumulation of several cholestanol-type steroidal saponins, confirming its function in the SGA pathway (Fig. 4B and fig. S6, F to I). Additionally, GAME6, encoded by another cluster gene, was previously suggested to be associated with SGA metabolism (*12*).

GAME4 and a putative transaminase (*GAME12*) that was highly coexpressed were positioned in close proximity to each other on chromosome 12 of both species (Fig. 3). Silencing *GAME4* in potato by RNA interference (RNAi) (*GAME4*i plants), showed a reduction by a factor of up to 74 in the levels of α-solanine/chaconine and other SGAs in both leaves and tubers (fig. S7, A to E). In the dark, normal quantities of α-solanine and α-chaconine are 200 and 370 mg/kg, respectively (fig. S7C). After light exposure, levels of α-solanine and α-chaconine increase in tuber skin, and quantities are 510 and 870 mg/kg, respectively. With the *GAME4* gene silenced, the concentrations of both α-solanine and α-chaconine remained below 5 mg/kg and did not change with light exposure (fig. S7, C to E).

In the domesticated tomato, the dominant SGA in leaves and mature green fruit is α-tomatine that was reduced by a factor of ~100 in *GAME4i* plants (figs. S7F and S8 and table S14). During the transition from green to red fruit, α-tomatine is converted to lycoperosides and esculeosides. These two classes of compounds represent hydroxylated, glycosylated, and often acetylated α-tomatine derivatives (*13*). Hence, reduced α-tomatine accumulation in the green fruit stage resulted in reduced accumulation of lycoperosides and esculeosides in the red-ripe fruit stage (fig. S7G). Complementary results were obtained in *GAME4*-overexpressing tomato plant leaves (*GAME4*oe), as they accumulated 2.5 times as much α-tomatine as the controls (fig. S8B). Furthermore, *GAME4*oe red-ripe fruit exhibited 2.9 times more esculeoside A (fig. S8C), demonstrating once more the central role of GAME4 in SGA biosynthesis. It appeared that SGA precursors [i.e., cholesterol, cycloartenol, and (S)-2,3-oxidosqualene] and the phytosterols campesterol and β-sitosterol accumulated in leaves of *GAME4*-silenced tomato plants (fig. S9). Despite altered phytosterol levels, *GAME4*-silenced plants were not affected in their morphology under the conditions examined in this study (*14*).

Tomato and potato *GAME4*i plants with decreased levels of SGAs accumulated nitrogen-lacking compounds identified as STSs (fig. S7, H and I, and fig. S10). Greater reduction in SGAs correlated with greater accumulation of STSs (fig. S7, D, E, H, and I). Levels of STSs were significantly induced by light in several wild-type and *GAME4*i lines examined (fig. S7, H and I). These results indicate that SGAs and STSs originate from the same precursor and that GAME4 is positioned in a branch point before the incorporation of nitrogen for SGA generation in the diverging biosynthetic pathways that produce these two classes of steroidal compounds (Fig. 1 and fig. S1).

GAME12 (transaminase)–silenced tomato leaves were found enriched with a furostanol-type saponin (Fig. 4D and fig. S6, J to M), suggesting additional hydroxylation of its accumulated substrate. We also

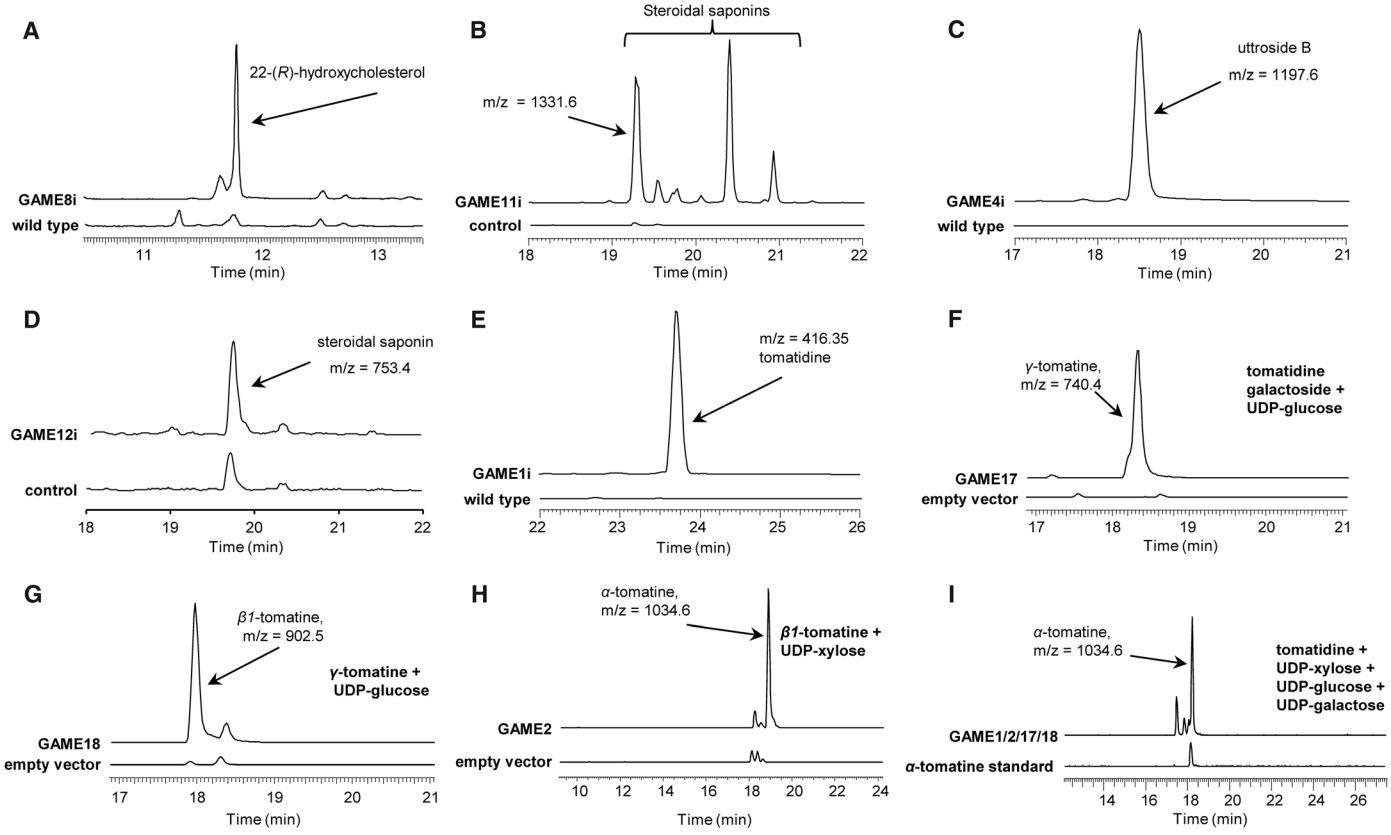

Fig. 4. Functional analysis of tomato GAME genes. (**A**) *GAME8*-silenced transgenic (RNAi) leaves accumulated 22-(*R*)-hydroxycholesterol compared to wild type. (**B**) An array of cholestanol-type steroidal saponins (STSs) accumulates in *GAME11* VIGS-silenced leaves. (**C**) An STS annotated as Uttroside B accumulates in *GAME4*-silenced transgenic leaves. (**D**) An STS [mass/charge ratio (*m/z*) = 753.4] accumulates in *GAME12* VIGS-silenced leaves. (**E**) Tomatidine, the steroidal alkaloid aglycone, accumulates in *GAME1*-silenced transgenic leaves. (**F** to **I**) Enzyme activity assays of the four recombinant tomato GAME glycosyltransferases (*14*). Reactions containing GAME17 (F) and GAME18 (G) recombinant proteins with UDP-glucose as donor-substrate, and T-Gal or T-Gal-Glu gama-tomatine as an acceptor-substrate, respectively, produced products with *m/z* = 740.4 and *m/z* = 902.5, respectively. Reaction products were identified as γ-tomatine for GAME17 (F) and T-Gal-Glu-Glu for GAME18 (G). Reaction containing β1-tomatine, the GAME2 recombinant protein, and UDP-xylose produced α-tomatine (H). Reaction containing tomatidine as substrate, UDP -galactose, -glucose and -xylose as sugar donors, and the GAME1, GAME2, GAME17, and GAME18 recombinant proteins resulted in accumulation of α-tomatine (I). See also figs. S5, S6, and S10.

functionally examined genes that were tightly coexpressed and positioned elsewhere in the genome that belong to the CYP72 subfamily of cytochrome P450s (i.e., GAME7 and GAME8). GAME7 was coexpressed in both species, whereas StGAME8a and StGAME8b were strongly coexpressed with *StSGT1* and *StGAME4* in potato. At present, we could not demonstrate SGA-related activity for GAME7, although as for GAME6, it was suggested to be involved in SGA metabolism (*12*). Yet, *GAME8*-silenced tomato leaves accumulated 22-(*R*)-hydroxycholesterol (fig. S6, N to Q), a proposed intermediate in the SGA biosynthetic pathway (Fig. 1).

The above findings allowed us to propose a pathway from cholesterol to α-tomatine. Cholesterol is hydroxylated at C22 by GAME7 (*12*), followed by GAME8 hydroxylation at the C26 position (Fig. 1). The 22,26-dihydroxycholesterol is then hydroxylated at C16 and oxidized at C22, followed by closure of the *E*-ring by GAME11 and GAME6 to form the furostanol-type aglycone. This order of reactions is supported by the accumulation of cholestanol-type saponins, lacking hydroxylation at C16 and the hemi-acetal *E*-ring when silencing *GAME11* (fig. S6, F to I). The furostanol-intermediate is oxidized by GAME4 to its 26-aldehyde, which is the substrate for transamination catalyzed by GAME12. Nucleophilic attack of the amino nitrogen at C22 leads to the formation of tomatidenol, which is dehydrogenated to tomatidine. Tomatidine is subsequently converted by GAME1 to T-Gal (*9*). T-Gal in its turn is glucosylated by GAME17 into γ-tomatine, which is further glucosylated by GAME18 to β1-tomatine that is finally converted to α-tomatine by GAME2 (Fig. 1).

Some specialized plant metabolites, particularly terpenoids, are the result of activities from clusters of genes (*15*, *16*). The existence of metabolic gene clusters raises questions about the advantages of such genomic organization (*17*). Reducing the distance between loci, resulting in coinheritance of advantageous combinations of alleles, may be one benefit of clustering (*17*). Clustering glycosyltransferases and core pathway genes, as observed here for SGAs, could maintain allelic combinations that support the metabolic outcome needed by the plant and reduce formation of phytotoxic aglycone compounds (*9*, *18*). We found that the regions of coexpressed genes in both chromosomes (i.e., 7 and 12) were flanked by similarly annotated genes and positioned identically along the genome, although poorly coexpressed with *GAME1*/*SGT1* and *GAME4* and likely not related to SGA metabolism (fig. S11 and table S13). This suggests a duplication event that facilitated the positioning alongside each other on chromosome 12 of *GAME4* and *GAME12*, both STSs and SGAs branch-point genes. Subsequent evolution of enzyme function of this gene pair likely allowed plants in the *Solanaceae* family to start producing the nitrogen-containing steroidal alkaloids.

We have shown that SGA levels can be severely reduced in potato tubers by modifying expression of an enzyme in the biosynthetic pathway. The lack of SGAs in such plants might make them sensitive to biotic stress, and the increased production of STSs (as occurred in *GAME4*-silenced plants)—which are nontoxic to warm-blooded species, including humans (*19*)—might provide a compensatory defense mechanism (*20*). The findings open the way for developing new strategies, through genetic engineering or more classical breeding programs, to reduce quantities of the antinutritional SGAs in key crops of the *Solanaceae*, including potato, tomato, and eggplant. At the same time, it provides a platform for studying the SGA and STS biosynthetic pathways, transport, and regulatory systems that control the production of thousands of these chemicals in specific plant lineages.

References and Notes

1. N. N. Narayanan, U. Ihemere, C. Ellery, R. T. Sayre, *PLoS ONE* **6**, e21996 (2011).
2. L. C. Dolan, R. A. Matulka, G. A. Burdock, *Toxins* **2**, 2289–2332 (2010).
3. L. L. Sanford, S. P. Kowalski, C. M. Ronning, K. L. Deahl, *Am. J. Potato Res.* **75**, 167–172 (1998).
4. M. Friedman, *J. Agric. Food Chem.* **54**, 8655–8681 (2006).
5. M. Desfosses, *J. Pharmacie* **6**, 374–376 (1820).
6. J. G. Roddick, *Phytochemistry* **28**, 2631–2634 (1989).
7. FDA Poisonous Plant Database, www.accessdata.fda.gov/scripts/Plantox/
8. K. F. McCue *et al.*, *Plant Sci.* **168**, 267–273 (2005).
9. M. Itkin *et al.*, *Plant Cell* **23**, 4507–4525 (2011).
10. E. Eich, *Solanaceae and Convolvulaceae: Secondary Metabolites: Biosynthesis, Chemotaxonomy, Biological and Economic Significance* (Springer, Berlin, 2008).
11. The Potato Genome Sequencing Consortium, *Nature* **475**, 189–195 (2011).
12. N. Umemoto, S. Katsunori, U.S. Patent application 20120159676 A1 (2012).
13. T. Yamanaka *et al.*, *J. Agric. Food Chem.* **57**, 3786–3791 (2009).
14. Materials and methods are available as supplementary materials on *Science* Online.
15. D. J. Kliebenstein, A. Osbourn, *Curr. Opin. Plant Biol.* **15**, 415–423 (2012).
16. T. Winzer *et al.*, *Science* **336**, 1704–1708 (2012).
17. A. E. Osbourn, *Plant Physiol.* **154**, 531–535 (2010).
18. B. Field, A. E. Osbourn, *Science* **320**, 543–547 (2008).
19. P. F. Dowd, M. A. Berhow, E. T. Johnson, *J. Chem. Ecol.* **37**, 443–449 (2011).
20. S. G. Sparg, M. E. Light, J. van Staden, *J. Ethnopharmacol.* **94**, 219–243 (2004).

Acknowledgments: We thank A. Tishbee and R. Kramer for operating the UPLC-qTOF-MS instrument and the European Research Council (SAMIT-FP7 program) for supporting the work in the A.A. laboratory. A.A. is the incumbent of the Peter J. Cohn Professorial Chair. J.B. was supported by the European Union 7th Frame Anthocyanin and Polyphenol Bioactives for Health Enhancement through Nutritional Advancement (ATHENA) Project (FP7-KBBE-2009-3-245121-ATHENA). U.H. was partially supported by fellowship AZ: I/82 754, Volkswagen Foundation, Hannover, Germany. We thank the Council of Scientific and Industrial Research (India) for support to A.P.G. (Raman Research Fellowship), A.J.B., Y.C., and P.S. (Research Fellowship) and the University Grants Commission (India) for supporting B.S. We also thank D. R. Nelson for assistance with CYP450 gene classification and R. Last for critically reading the manuscript. A.A. and M.I. are inventors on publication number WO2012095843 A1, submitted by Yeda Research and Development Co. Ltd, which covers the use of the *GAME4* gene for generating low-alkaloid fruit and tubers.

Supplementary Materials

www.sciencemag.org/cgi/content/full/science.1240230/DC1
Materials and Methods
Figs. S1 to S15
Tables S1 to S16
References (*21*–*31*)

8 May 2013; accepted 6 June 2013
Published online 20 June 2013;
10.1126/science.1240230

Genome-Wide Comparison of Medieval and Modern *Mycobacterium leprae*

Verena J. Schuenemann,[1]* Pushpendra Singh,[2]* Thomas A. Mendum,[3]* Ben Krause-Kyora,[4]* Günter Jäger,[5]* Kirsten I. Bos,[1] Alexander Herbig,[5] Christos Economou,[6] Andrej Benjak,[2] Philippe Busso,[2] Almut Nebel,[4] Jesper L. Boldsen,[7] Anna Kjellström,[8] Huihai Wu,[3] Graham R. Stewart,[3] G. Michael Taylor,[3] Peter Bauer,[9] Oona Y.-C. Lee,[10] Houdini H.T. Wu,[10] David E. Minnikin,[10] Gurdyal S. Besra,[10] Katie Tucker,[11] Simon Roffey,[11] Samba O. Sow,[12] Stewart T. Cole,[2]† Kay Nieselt,[5]† Johannes Krause[1]†

Leprosy was endemic in Europe until the Middle Ages. Using DNA array capture, we have obtained genome sequences of *Mycobacterium leprae* from skeletons of five medieval leprosy cases from the United Kingdom, Sweden, and Denmark. In one case, the DNA was so well preserved that full de novo assembly of the ancient bacterial genome could be achieved through shotgun sequencing alone. The ancient *M. leprae* sequences were compared with those of 11 modern strains, representing diverse genotypes and geographic origins. The comparisons revealed remarkable genomic conservation during the past 1000 years, a European origin for leprosy in the Americas, and the presence of an *M. leprae* genotype in medieval Europe now commonly associated with the Middle East. The exceptional preservation of *M. leprae* biomarkers, both DNA and mycolic acids, in ancient skeletons has major implications for palaeomicrobiology and human pathogen evolution.

Leprosy, which results from infection with the unculturable pathogen *Mycobacterium leprae*, was common in Europe until the 16th century, when it essentially disappeared. In contrast, disease prevalence has remained high in the developing world. During the past 20 years,